Experimental Verification of High Frequency Link DC-AC Converter using Pulse Density Modulation at Secondary Matrix Converter.

Jun-ichi Itoh, Ryo Oshima and Hiroki Takahashi
Dept. of Electrical, Electronics and Information Engineering
Nagaoka University of Technology
Nagaoka, Niigata, Japan
ryo_oshima@stn.nagaokaut.ac.jp

***Abstract*— This paper verifies an isolated DC-AC power converter using a single phase to three phase matrix converter in experiment. A matrix converter does not require the large reactors and the large smoothing capacitors in a DC-link part. Furthermore, the proposed control method enables zero voltage switching of the matrix converter by implementing a phase shift control on the primary inverter and a pulse density modulation on the secondary matrix converter. In this paper, the fundamental operation of the converter is demonstrated by the experiment. From the experimental results, the total harmonic distortion in the output voltage is less than 5% in the entire range. In addition, a maximum efficiency of 90.9 % is achieved at an output power of 1.5kW.**

Keywords*— *dc-ac converter, high frequency link converter, pulse density modulation, zero voltage switching.

I. INTRODUCTION

Recently, from the view point of global warming and environmental problems, the renewable energy systems are focused on. However, in a renewable energy system, especially a wind turbine and a photovoltaic cell, a power fluctuation occurs owing to the meteorological conditions. Therefore, an energy storage system using a battery is necessary in order to suppress the power fluctuation.

The battery energy storage system requires a DC-AC converter to connect the grid and the battery. In addition, the DC-AC converter requires the isolation by a transformer in order to protect the system from failure and noise. However, an isolation transformer designed for the commercial frequency is bulky and heavy. Hence, in order to reduce the volume of the isolation transformer, a high frequency AC link converter has been researched.

In past works, two typical high frequency link DC-AC converter topologies have been proposed. First one consists of a high frequency isolated DC-DC converter and a three-phase inverter for the grid connection [1-4]. This circuit configuration reduces the volume of the isolation transformer because the full bridge inverter operates in the DC-DC converter at the high frequency. However, the DC link capacitors between the rectifier and three-phase inverter are bulky in order to smooth the DC link voltage. Thus, it is difficult to reduce the volume of the system and to realize long lifetime. Moreover, the total efficiency decreases because of three times power conversion.

Second one is the high frequency link converter with a matrix converter for the secondary power conversion in order to reduce the volume of the capacitor [5-7]. This circuit topology has advantages as follows: (i) the number of power conversion is reduced to two times. Thus, the efficiency is higher than the former type. (ii) The system achieves smaller size and long lifetime because the DC-link capacitor is not required. However, when PWM (pulse width modulation) control is used to the matrix converter in the secondary side, the switching loss of the matrix converter is increased because of a hard switching. Moreover, the conduction loss of the inverter is increased because the freewheeling current flows at the inverter while the matrix converter outputs zero vectors.

This paper proposes an isolated DC-AC converter which adopts a matrix converter with pulse density modulation (PDM) and the suppression control of freewheeling current. By using the PDM, zero voltage switching (ZVS) is achieved. Then, the fundamental operation of the proposed circuit is demonstrated in the simulations and the experiments. The remainder of this paper is organized as follows. First, the circuit configuration of the high frequency link converter is described. Second, the control scheme is explained in detail. Third, a problem of freewheeling current occurs at the primary inverter and the suppression control of freewheeling current are explained. Fourth, a fundamental operation of the proposed method is shown in simulation. Finally, the operation of the proposed circuit is demonstrated under the condition of an input DC voltage of 200 V and an AC link frequency of 50 kHz. In addition, the efficiency and the total harmonic distortion (THD) of the output voltage are evaluated in order to clarify the validity of the proposed system.

II. CIRCUIT CONFIGURATION

Fig. 1 shows the configuration of the conventional circuit. The conventional circuit comprises a bidirectional DC-DC converter with an isolation transformer such as dual active bridge converter [8-9]. However, the two-stage topology requires the bulky DC capacitors in order to smooth the DC link voltage.

Fig. 2 shows the main circuit configuration of the proposed DC-AC converter with the matrix converter. The proposed circuit comprises a full bridge inverter with phase shift control at the primary side of the transformer and the single-phase to three phase matrix converter at the secondary side. It is noted that the PDM is applied to the matrix converter only. The proposed system achieves high efficiency because the number of the power conversions is reduced owing to the matrix converter. In addition, the advantages of the matrix converter are long lifetime and the reduced volume owing to the absence of the large DC-link capacitor and an initial charge circuit. However, it is difficult to reduce the switching loss due to the hard switching when the conventional PWM method is applied to the matrix converter.

In order to reduce the switching loss of the matrix converter by implementation of ZVS, the PDM is applied to the matrix converter. In addition, for simplicity of the PDM, the primary inverter provides three-level voltage including zero voltage with the phase shift control. As a result, the matrix converter achieves ZVS when the switches turn in the zero voltage periods and a commutation scheme of the matrix converter is simplified.

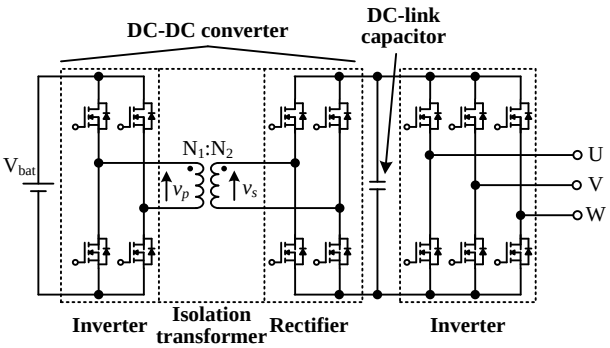

Fig.1. High frequency link DC-AC converter with rectifier and inverter

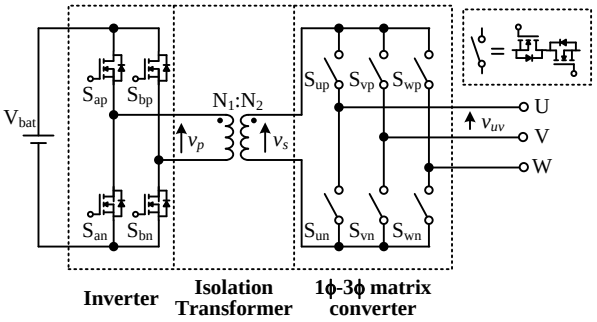

Fig.2. High frequency link DC-AC converter with matrix converter

III. CONTROL STRATEGIES

A. Phase shift control

Fig. 3 shows a control block diagram of the phase shift control for the primary inverter. This control is composed of a carrier generator, a phase delay circuit, and two comparators. Duty ratio D of the primary inverter to adjust the input voltage of the matrix converter is controlled by the phase delay.

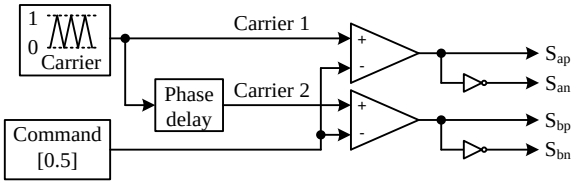

Fig.3. Control block diagram of the inverter.

Fig. 4 shows an operation principle of the phase shift control for the primary inverter. The inverter outputs three-level voltage including zero voltage by the phase shift control. Therefore, the matrix converter achieves ZVS if the matrix converter turns in the zero voltage period generated by the primary inverter. Actually, the phase delay is achieved by adjusting carrier delay time T_{PD} given by (1).

$$T_{PD} = \frac{D}{2 \times f_{c\_inv}} \quad \cdots\cdots(1)$$

where, f_{c_inv} is carrier frequency of the primary inverter.

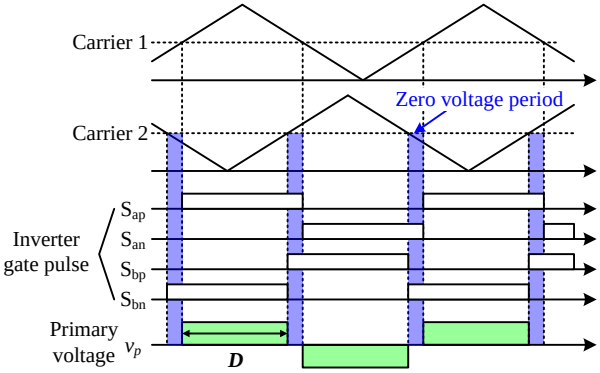

Fig.4. Operation principle of the phase shift control for the primary inverter.

B. Pulse density modulation method based on space vector modulation

Fig. 5 shows a control block diagram of a PDM for the matrix converter. This control is composed of space vector modulation (SVM), a clock (CLK) generator for

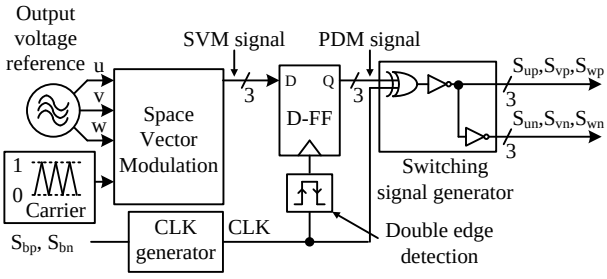

Fig.5. Control block diagram of the matrix converter.

the PDM, a delay (D-FF) and a switching signal generator. In order to generate the gate signal by the PDM, the D-FF is used to quantize the duty references generated by the SVM. Moreover, the CLK to drive the D-FF is synchronized with the zero voltage periods owing to the phase shift control in order to achieve the PDM and ZVS easily.

Fig. 6 shows operation waveforms of the PDM which enables ZVS of the matrix converter. The PDM controls the density and the pole of the constant width pulse. In addition, these pulse signals are used as the minimum unit of the output voltage waveform [10]. It should be noted that the input voltage of the matrix converter (secondary voltage of the transformer) is high frequency square waveform. Therefore, a half cycle of the input voltage is used as one pulse of the PDM. Then, the half cycle period of the input voltage is detected easily by the gate pulses S_{bp} and S_{bn} of the primary inverter. As a result, the PDM and the ZVS of the matrix converter are implemented without switching loss by the control scheme in Fig. 5.

IV. SUPPRESSION CONTROL OF FREEWHEELING CURRENT

This chapter describes a problem and the principle of a freewheeling current mode at the primary side. In addition, a suppression control of freewheeling current is presented in order to improve system efficiency.

Fig. 7 shows operation modes of the DC-AC converter. The red line (state 1) in Fig. 7(a) shows a current path when the primary inverter outputs positive voltage and the matrix converter selects (100) vector. It should be noted that this case is not the freewheeling current mode. In the state 1, the transformer current contributes to provide the DC battery power to the load because the primary inverter outputs positive voltage.

In Fig. 7(b), the red line shows a current pathway when the matrix converter chooses a vector except the zero vector though the primary inverter outputs zero voltage. This paper defines this mode as the freewheeling current mode. The problem of the freewheeling current mode means increasing conduction loss of the primary inverter and copper loss of the transformer. The principle of the increasing losses is following. In this state, the DC battery power is not transmitted to the load because the primary inverter outputs zero voltage. However, the primary and the secondary current of the transformer flow since the matrix converter selects a vector not the zero vector and the load is inductive. As a result, a current pathway in the primary side is constructed and the conduction loss of the primary inverter and the copper loss of the transformer are generated although the transmitted power from the DC battery to the load is zero. Therefore, the freewheeling current mode needs to be suppressed in order to improve the system efficiency.

Fig. 7(c) shows the principle of the suppression method of the freewheeling current mode. The

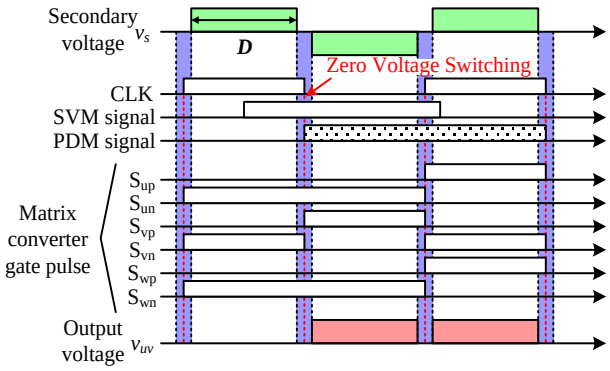

Fig.6. Operation principle of the pulse density modulation for the matrix converter.

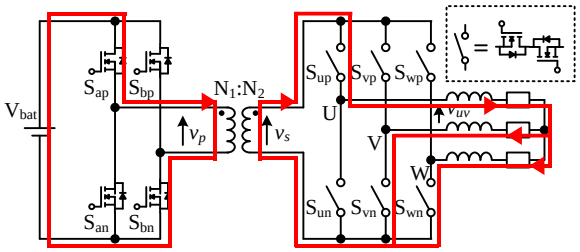

(a) The output current pathway when the DC-AC converter supplies electric power from the source to the RL load. (State 1)

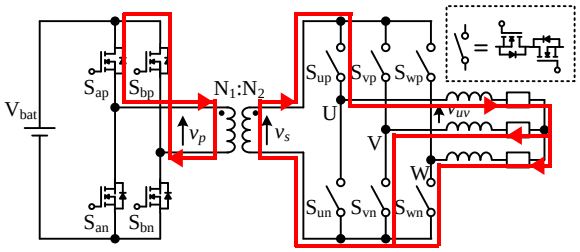

(b) The current pathway when the matrix converter supplies electric power while the inverter outputs zero vector. (State 2)

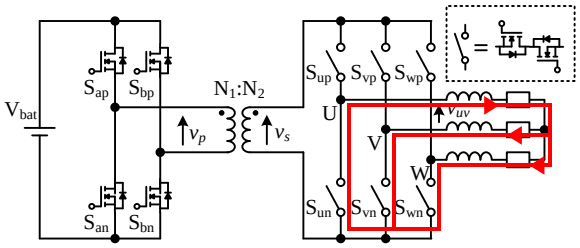

(c) The current pathway after changed the output current pathway. (State 3)

Fig.7 Switching transition of the DC-AC converter

TABLE I
SIMULATION AND EXPERIMENTAL CONDITIONS

Element	Symbol	Value
Battery voltage	V_{bat}	200 V
Carrier frequency of inverter	f_{c_inv}	50 kHz
Carrier frequency of matrix converter	f_{c_mc}	5 kHz
Modulation frequency of matrix converter	f_{m_mc}	50 Hz
Turn ratio	N_1:N_2	1:2
Duty of primary voltage	D	0.9 p.u.
Load power	P_{load}	3 kW

suppression method focuses on the output voltage in the freewheeling current mode. In Fig. 7 (b), the output voltage is zero because the primary inverter outputs zero voltage though the matrix converter chooses a vector except the zero vector. Therefore, the freewheeling current mode is equivalent to the zero vector of the matrix converter. In addition, if the matrix converter selects the zero vector, the secondary current of the transformer does not flow. It results in reducing the conduction loss of the primary inverter and the copper loss of the transformer. Hence, in order to prevent the freewheeling current mode, the matrix converter should select the zero vector while the primary inverter outputs zero voltage such as Fig. 7 (c).

V. SIMULATION RESULTS

Table I lists the simulation parameters. The DC-AC converter outputs three-phase voltage of 200V and 50 Hz for the grid connection. However, the simulation is implemented with a RL load for simplicity.

Fig. 8 shows the input and output waveforms of the matrix converter with the proposed method in simulations. It should be noted that the cut-off frequency of the low pass filter to observe the output voltage waveform is 1 kHz. As shown in figure, it is confirmed that the output current of the matrix converter is sinusoidal waveform. Then, the output current THD is 2.79%.

Fig. 9 shows the enlarged waveform of Fig. 8. The secondary voltage of the transformer is three-level voltage of 50 kHz. In addition, the output voltage waveform consists of the secondary voltage pulses of the transformer and the density of the pulses is controlled by the PDM. Thus, the operation of the PDM in the matrix converter is confirmed.

Fig. 10 shows the efficiency characteristic for the output power in simulation. It is noted that this loss simulation calculates only semiconductor losses on the proposed circuit. The efficiency is 97.8% at the maximum point. Moreover, the efficiency is greater than 95% in the entire range. Therefore, it is confirmed that the high efficiency is obtained by ZVS.

VI. EXPERIMENTAL RESULTS

A. Fundamental operation

In order to confirm the fundamental operation of the proposed method, the proposed circuit is demonstrated with the 3-kW prototype circuit in experiment. The experimental conditions are same as the simulation.

Fig. 11 shows the input and output waveforms of the matrix converter in experiment. As the result, the output current is sinusoidal and the output current THD is obtained by 4.28%.

Fig. 12 shows the enlarged waveforms of Fig. 11ff. From the result, it is confirmed that the secondary voltage of the transformer is 50kHz and three-level, which has

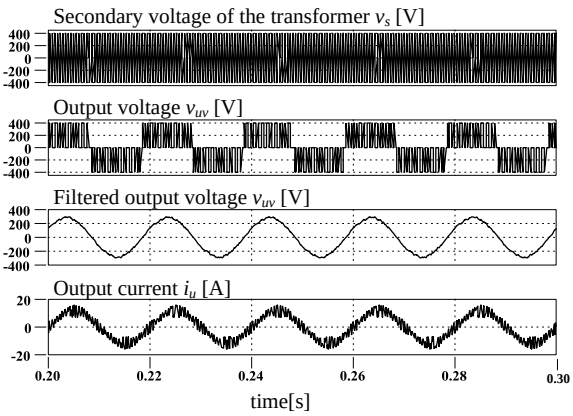

Fig.8. The input and output waveforms of the secondary matrix converter in simulation.

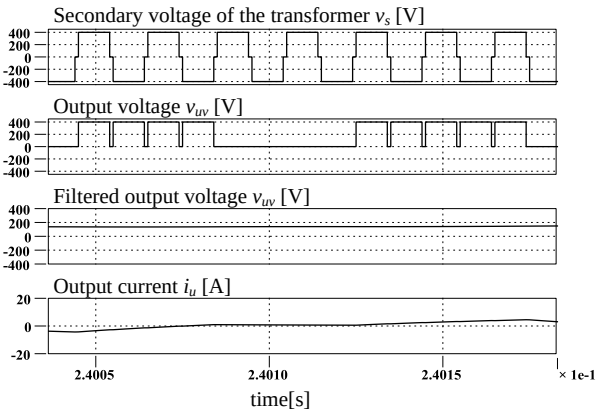

Fig.9. Enlarged waveforms of Fig.8.

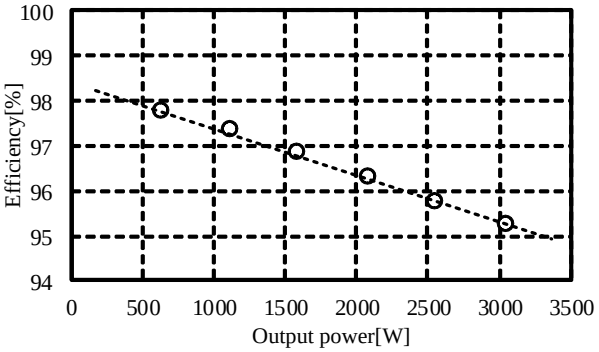

Fig.10. Efficiency characteristics except the transformer obtained from R-L load experiment that is subjected to the output power in simulation.

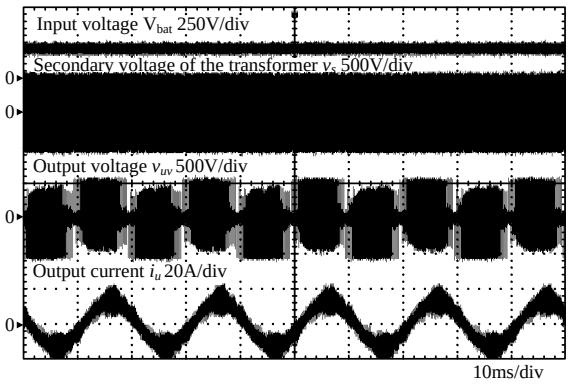

Fig.11. Experimental waveforms of input and output of the DC-AC converter.

the zero voltage period. In addition, the output voltage waveform consists of the secondary voltage pulses of the transformer. Moreover, the density of the pulse is controlled by the PDM. Thus, the PDM of the matrix converter is confirmed.

Fig. 13 shows the ZVS operation of the matrix converter in the proposed system. From the results, when the secondary voltage of the transformer is zero voltage, the switching of the matrix converter is implemented and the ZV is achieved.

Fig. 14 shows output voltage THD characteristic for the output power. As shown in Fig. 13, the output voltage THD is 3.76% at the minimum point and less than 5% all of the output power range. Therefore, the proposed system can be connected to the grid if the interconnection inductors are set to several percent of the rated power capacity.

B. Effectiveness of the suppression control of freewheeling current

Fig. 15 shows the primary voltage and current of the transformer regarding the suppression control of the freewheeling current mode in experiment. Fig. 15 (a) shows a result without the suppression control and Fig. 15 (b) shows a result with the control. It should be noted that the duty ratio D of the primary inverter is set to 0.5 p.u. to observe its difference easily. From Fig. 15 (a), the primary current flows while the primary inverter outputs zero voltage because of the freewheeling current mode. However, as shown Fig. 15 (b), the primary current of the transformer does not flow during the zero voltage period because the suppression control forces the matrix converter to select the zero vector while the primary inverter provides zero voltage. The voltage and current fluctuation in Fig. 15 is caused by a LC resonance due to the capacitance between primary side and secondary side of the transformer and wiring inductance.

Fig.16 shows the efficiency characteristic with respect to the output power with RL loads. A dotted line shows the efficiency characteristic with the suppression control of freewheeling current and the solid line shows efficiency characteristic with the suppression method. From the results, the efficiency without the suppression control of freewheeling current mode is 89.8% at maximum point. However, the suppression control of freewheeling current improves the efficiency. The maximum efficiency with the suppression control is obtained by 90.9 %. Especially, the suppression control is more effective in light load region because the exciting current of transformer is reduced. Therefore, the suppression control of the freewheeling current improves the efficiency of 4.4% at a maximum. Thus, the validity of the suppression control of the freewheeling current mode is confirmed.

Fig.17 shows loss analysis results at the maximum efficiency point and the rated power in experiment with the suppression control of freewheeling current. Then, the

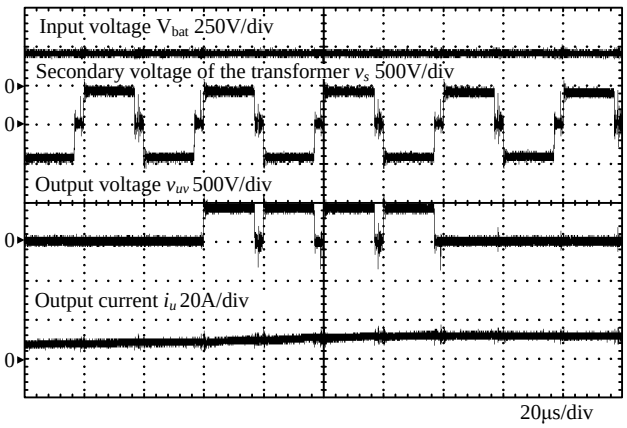

Fig.12. Enlarged waveforms of Fig.10.

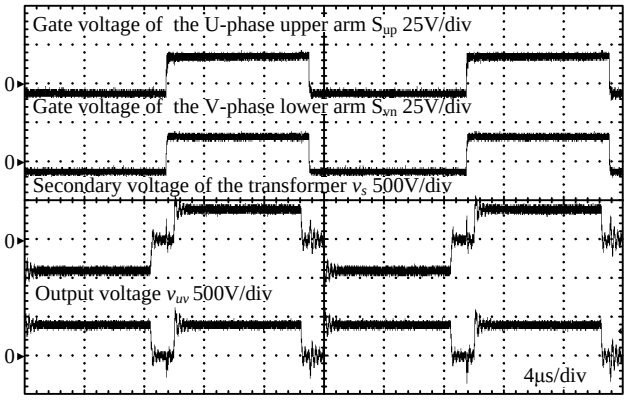

Fig.13. Experimental waveforms when the gate signals are changed in the zero voltage period.

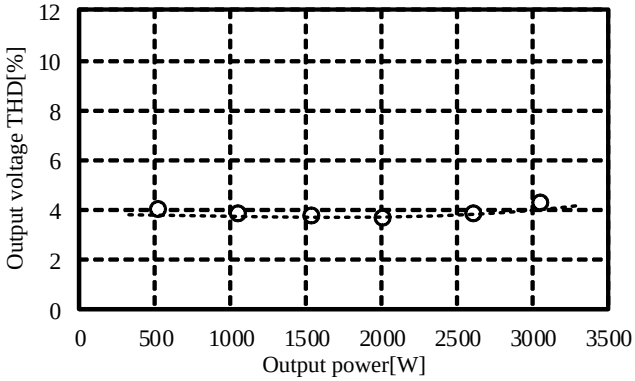

Fig.14. THD characteristics of output voltage obtained from R-L load experiment that is subjected to the output power.

rated power is 3kW and the maximum efficiency is obtained at 1.5kW.

It should be noted that matrix converter loss includes the snubber loss. Then, snubber voltage is 880V at the rated power because the snubber absorbs the leakage inductance energy of the transformer and commutation failure of the matrix converter. As a result, the snubber loss is obtained by 12.9W and accounts for 35% of the matrix converter loss. However, if the commutation sequence is modified, it is possible to reduce the snubber loss because the snubber voltage increase is suppressed. Consequently, the efficiency improvement of DC-AC converter will be expected.

On the other hand, the main loss of the DC-AC

converter is the inverter loss at both maximum efficiency point and the rated power. Therefore, it is necessary to reduce the inverter loss in order to improve the efficiency of the DC-AC converter. As a method to increase the efficiency, soft switching technique will be introduced in the future.

VII. CONCLUSION

This paper verified the isolated DC-AC converter using a matrix converter in simulations and experiments. The matrix converter in the proposed system employs the PDM and achieves ZVS by combination with the high frequency inverter with the phase shift control. From the simulation result, it is confirmed the fundamental operation and the maximum efficiency of proposed DC-AC converter of 97.8% is obtained. In addition, a 3-kW prototype of the proposed circuit was tested. From the experimental results, the ZVS operation and the PDM of the matrix converter were confirmed. Moreover, the output voltage THD is less than 5% in the entire range.

Besides, the efficiency characteristics with respect to the output power is evaluated. In addition, a loss analysis of the experimental result is implemented. A maximum efficiency of 90.9 % is achieved at 1.5kW output power with the suppression control of freewheeling current. It is confirmed that the efficiency of 1 % is improved by applying the suppression control of freewheeling current. And, from the loss separation results, the inverter loss is the main loss of the DC-AC converter.

In the future work, in order to achieve the high efficiency of DC-AC converter, it will be performed the soft switching at the inverter. Finally, the prototype circuit will be connected to the grid and evaluated in experiment.

REFERENCES

[1] H. Ertl, J. W. Kolar, and F. C. Zach, "A novel multicell DC-AC converter for applications in renewable energy systems," IEEE Trans. Ind. Electron., vol. 49, no. 5, pp. 1048–1057, 2002.

[2] R. P. Torrico-Bascope, D. S. Oliveira, Jr., C. G. C. Branco, and F. L.M. Antunes, "A UPS with 110-V/220-V input voltage and high-frequency transformer isolation," IEEE Trans. Ind. Electron., vol. 55, no. 8, pp.2984–2996, 2008.

[3] C. Rodriguez and G. Amaratunga, "Long-lifetime power inverter for photovoltaic AC modules," IEEE Trans. Ind. Electron., vol. 55, no. 7, pp. 2593–2601, 2008.

[4] R. P. T. Bascope, D. S. Oliveira, C. G. C. Branco, and F. L. M. Antunes, "A UPS with 110 V/220 V input voltage and high-frequency transformer isolation," IEEE Trans. Ind. Electron., vol. 55, no. 8, pp. 2984–2996, Aug. 2008.

[5] I. Yamato, N. Tokunaga, Y. Matsuda, Y. Suzuki, and H. Amaro, "High frequency link dc–ac converter for UPS with a new voltage clamper," in Proc. IEEE Power Electron. Spec. Conf., pp. 749–756, 1990.

[6] K. Inagaki, T. Furuhashi, A. Ishiguro, M. Ishida, S. Okuma, Y. Uchikawa, "A Waveform Control Mehod of AC to DC converters with High-Frequency Links," IEEJ Trans. D,Vol.110, No.5, pp.525-533, 1990.

[7] K. Inagaki and S. Okuma, "High frequency link DC/AC converters using three phase PWM cycloconverters for

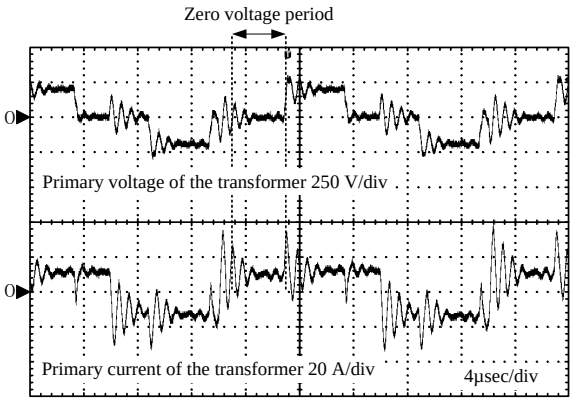

(a) Without the suppression control of freewheeling current.

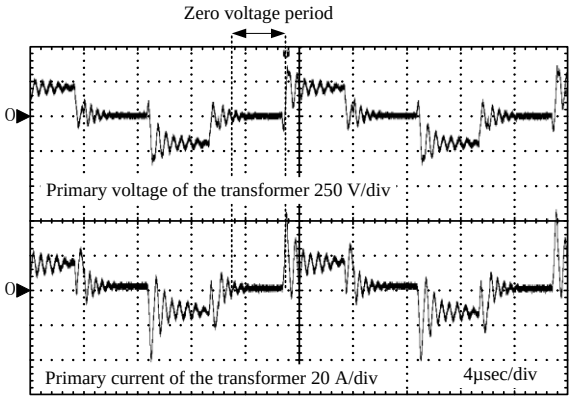

(b) With the suppression control of freewheeling current.

Fig.15 Experimental waveforms of primary voltage and current of the transformer with the suppression control of freewheeling current.

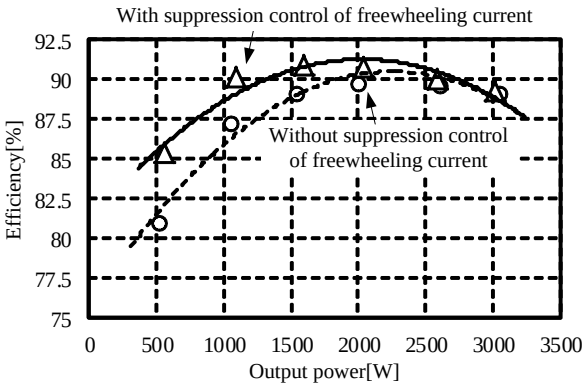

Fig.16 efficiency characteristics of the DC-AC converter obtained from R-L load experiment that is subjected to the output power.

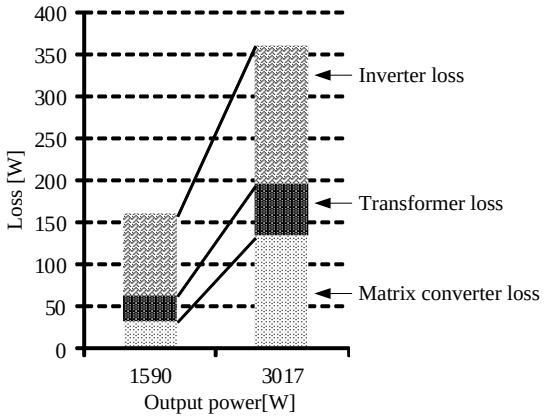

Fig.17 Loss analysis results of the DC-AC converter with the suppression control of freewheeling current.

uninterruptable power supplies," in Proc. Telecommun. Energy Conf., pp. 580–586, 1991.

[8] H. Bai and C. Mi, "Eliminate reactive power and increase system efficiency of isolated bidirectional dual-active-bridge dc–dc converters using novel dual-phase-shift control," IEEE Trans. Power Electron., vol. 23, no. 6, pp. 2905–2914, 2008.

[9] A. K. Jain and R. Ayyanar, "PWM control of dual active bridge: Comprehensive analysis and experimental verification," in Proc. 34th IEEE IECON, Orlando, FL, Nov. 10–13, pp. 909–915, 2008.

[10] Y. Nakata, J. Itoh, "Pulse Density Modulation Control using Space Vector Modulation for a Single-phase to Three-phase Indirect Matrix Converter," IEEE ECCE 2012, Raleigh, P3905, pp. 1753-1759, 2012.